Curl-free positive definite form of time-harmonic Maxwell's equations well-suitable for iterative numerical solving

OPEN ACCESS
IOP Publishing
Plasma Physics and Controlled Fusion
Plasma Phys. Control. Fusion **63** (2021) 124007 (6pp)
https://doi.org/10.1088/1361-6587/ac32a4

Curl-free positive definite form of time-harmonic Maxwell's equations well-suitable for iterative numerical solving

V E Moiseenko[1,*] **and O Ågren**[2]

[1] Institute of Plasma Physics, National Science Center 'Kharkiv Institute of Physics and Technology', 61108 Kharkiv, Ukraine
[2] Uppsala University, S-75108 Uppsala, Sweden

E-mail: moiseenk@ipp.kharkov.ua

Received 17 August 2021, revised 8 October 2021
Accepted for publication 22 October 2021
Published 15 November 2021

Abstract

A new form of time-harmonic Maxwell's equations is developed on the base of the standard ones and proposed for numerical modeling. It is written for the magnetic field strength **H**, electric displacement **D,** vector potential **A** and the scalar potential Φ. There are several attractive features of this form. The 1st one is that the differential operator acting on these quantities is positive. The 2nd is absence of curl operators among the leading order differential operators. The Laplacian stands for leading order operator in the equations for **H, A** and Φ, while the gradient of divergence stands for **D**. The 3rd feature is absence of space varied coefficients in the leading order differential operators that provides diagonal domination of the resulting matrix of the discretized equations. A simple example is given to demonstrate the applicability of this new form of time-harmonic Maxwell's equations.

Supplementary material for this article is available online

Keywords: Maxwell's equations, vector and scalar potentials, electric and magnetic field

1. Introduction

Time-harmonic Maxwell's equations are used for modeling electromagnetic field interaction with media in many sciences, e.g. biology, medical science, etc. In plasma physics, the main area of their application is radio-frequency (RF) plasma heating. RF heating is used both in low and high temperature plasma. The peculiar feature of the plasma response on electromagnetic field is its complexity. Another important thing is the geometry of the magnetic field which confines plasma. The last feature requires multi-dimensional modeling, 2D and 3D. These features give life to plasma-specific electromagnetic phenomena, such as wave branches with very different space scale, kinetic waves which behavior is strongly influenced by plasma temperature, mode conversion in non-uniform plasma, geometry-induced modes, etc. This all is modeled using time-harmonic Maxwell's equations.

The conventional form of time-harmonic Maxwell's equations in non-magnetic media is:

$$\nabla \times \mathbf{E} = ik_0 \mathbf{H};\ \nabla \times \mathbf{H} = -ik_0 \hat{\varepsilon} \cdot \mathbf{E} + \frac{4\pi}{c} \boldsymbol{j}_{\text{ext}} \qquad (1a,b)$$

where **E** and **H** are electric and magnetic field strengths, $\hat{\varepsilon}$ is the dielectric tensor, $\mathbf{j}_{\text{ext}}$ is the external (antenna) current

* Author to whom any correspondence should be addressed.

density, $k_0 = \omega/c$, c is the speed of light and the time dependence of all quantities is realized through the multiplier $\exp(-i\omega t)$. With proper boundary conditions, such equations are relevant for problems of RF wave excitation and propagation in plasmas and other media. For finite element analysis, the 1st order equations (1*a*,*b*) are often combined into the form:

$$\nabla \times \nabla \times \mathbf{E} = k_0^2 \hat{\varepsilon} \cdot \mathbf{E} + \frac{4\pi i\omega}{c^2} \boldsymbol{j}_{\text{ext}}, \tag{2}$$

in which the leading derivatives are of 2nd order.

Numerical solution of the boundary problem normally implies the discretization in space. The *curl* operator has some features which are not always reproduced after the discretization: e.g. it has zero-valued eigenvalue, and the eigenvectors are gradients of different scalar functions. The applied standard discretization technique born spurious modes, both for equations (1*a*,*b*) as well as equation (2). Since $\nabla \cdot \nabla \times \mathbf{F} = 0$ (for any arbitrary vector $\mathbf{F}$), a set of the components of the *curl* operator is degenerate. The degeneration is cancelled by the discretization procedure, and a new wave-like spurious mode appears which has no physical nature. To avoid this, a number of methods have been proposed. The 1st one is the Yee template for the finite differences [1]. In this template the mesh is staggered, and every **E**- and **H**-field component occupies different mesh nodes. This introduces difficulties for imposing the boundary conditions, calculation of dissipated power, and reproducing correctly rotating electric field components, $E_{\pm} = E_x \pm E_y$, which are responsible for the cyclotron wave dumping in magnetized plasma (the steady magnetic field is in z direction). For equation (2) a special template has been proposed [2] and used in [3, 4] with the same mesh for all components of the electric field. These two templates produce degenerate systems, and the spurious modes do not appear.

The Yee approach has a finite element analog, a Gruber–Rappaz method [5]. This method uses different order Lagrange and Hermite finite elements for different components of the electric field. Later on, special curl-conforming finite elements were invented like Nedelec finite elements [6].

Maxwell's equations in an alternative form can be obtained by introducing the vector and scalar potentials substituting $\mathbf{E} = ik_0\mathbf{a} - \nabla\phi$ and $\mathbf{H} = \nabla \times \mathbf{a}$ yield with the Coulomb gauge $\nabla \cdot \mathbf{a} = 0$:

$$\Delta\mathbf{a} + k_0^2 \hat{\varepsilon} \cdot \mathbf{a} + ik_0 \hat{\varepsilon} \cdot \nabla\phi = -\frac{4\pi}{c} \boldsymbol{j}_{\text{ext}} \tag{3}$$

$$\nabla \cdot [\hat{\varepsilon} \cdot (ik_0\mathbf{a} - \nabla\phi)] = 4\pi\rho_{\text{ext}} \tag{4}$$

where ρ_{ext} is the electric charge. Here and further on, the Laplacian of a vector is understood as $\Delta\mathbf{F} = \nabla\nabla \cdot \mathbf{F} - \nabla \times \nabla \times \mathbf{F}$. The form (3), (4) has no degenerate operators and can be discretized in a standard way which is a serious benefit.

After discretization a system of linear algebraic equations $\mathbf{Mx} = \mathbf{b}$ appears that could be solved by direct or iterative methods. All the above forms of the Maxwell's equations are sign indefinite and produce sign indefinite matrices, i.e. the scalar product (**f**, **Mf**) could have any value (here **f** is an arbitrary vector of the domain).

1D problem produces a dense band matrix and is best for direct methods. 2D and 3D problems result in sparse matrices. It is comfortable to use direct solvers since they can be applied to sign indefinite systems. The project PARDISO (Partial Differential Solver) should be mentioned here since is offers mostly universal and efficient tools for numerical solving (www.pardiso-project.org/). However, factorization unavoidably leads to matrix fill-in and increase of memory requirements. These requirements could be orders of magnitude higher than for initial sparse matrix.

The iterative methods are much more economic in memory. For sign indefinite linear problems we cannot apply iterative methods of relaxation family and the conjugate gradients (CGs) methods which otherwise offer good convergence rates. The GMRes, BiCGStab [7] and other methods are developed for this. The iterations for Maxwell's equations do not show good convergence and often stagnate [8]. The inner and outer iterations are used to avoid this [9], but performance of the iterations is still low. An expensive, but robust approach is to retain time dependence in Maxwell's equations while the problem is essentially time-harmonic [10].

The aim of the paper is to develop sign definite form of Maxwell's equations, discretization of which likely results in sign definite matrix for linear equations and allows one to use efficient iterations to obtain the numerical solutions. Another aim is to eliminate the *curl* operator at leading derivatives. This facilitates and simplifies the discretization and likely boosts the iterations.

2. New alternative form of Maxwell's equations

The source equations for this study are basically equations (1) written in the following form:

$$\nabla \times \mathbf{A} - ik_0\mathbf{H} = 0, \tag{5}$$

$$\nabla \times \mathbf{H} + ik_0\mathbf{D} = \frac{4\pi}{c} \boldsymbol{j}_{\text{ext}}, \tag{6}$$

$$\nabla \cdot \mathbf{D} = 4\pi\rho_{\text{ext}}, \tag{7}$$

$$\nabla\Phi + ik_0 \hat{\boldsymbol{\zeta}} \cdot \mathbf{D} - ik_0\mathbf{A} = 0, \tag{8}$$

where **D** is the electric displacement, $\mathbf{A} = ik_0\mathbf{a}$ and $\Phi = -i\phi/k_0$ are normalized potentials. The introduction of these normalized potentials is made to make all the quantities in the equations (5)–(7) of the same order of magnitude. This is done having in mind further discretization and combination of all discretized values to the single vector **x** of the linear system. The material equation is $\hat{\boldsymbol{\zeta}} \cdot \mathbf{D} = \mathbf{E}$ instead of the commonly used $\mathbf{D} = \hat{\varepsilon} \cdot \mathbf{E}$. This change is motivated by the want to have no coefficients before the differential operators of a leading order in (5)–(8).

With charge continuity assumed to be met, equations (5)–(7) are dependent since equation (7) can be obtained from

equation (5). This should be kept in mind during the further transforms.

Let us denote the left hand sides of the equations (5)–(8) as $\mathbf{L}_\mathrm{A}$, $\mathbf{L}_\mathrm{H}$, L_D and $\mathbf{L}_\Phi$, and right hand sides as $\mathbf{R}_\mathrm{H}$ and R_D. Then we construct the following quadratic form:

$$Q = \int \mathrm{d}V\,[\mathbf{L}_\mathrm{A}^* \cdot \mathbf{L}_\mathrm{A} + \mathbf{L}_\mathrm{H}^* \cdot (\mathbf{L}_\mathrm{H} - \mathbf{R}_\mathrm{H}) + L_\mathrm{D}^*(L_\mathrm{D} - R_\mathrm{D}) + \mathbf{L}_\Phi^* \cdot \mathbf{L}_\Phi]. \quad (9)$$

This form is zero valued if the operators $\mathbf{L}$ act on the solution of the system (5)–(7). Q is real and positive if $\mathbf{R}_\mathrm{H} = 0$ and $R_\mathrm{D} = 0$, and **A, H, D** and Φ are arbitrary. Using Gauss's theorem, Q is transformed into:

$$Q = Q_\mathrm{S} + Q_\mathrm{V}. \quad (10)$$

The surface term reads:

$$Q_\mathrm{S} = \int \mathrm{d}\mathbf{S} \cdot (\mathbf{A}^* \times \mathbf{L}_\mathrm{A}) + \int \mathrm{d}\mathbf{S} \cdot [\mathbf{H}^* \times (\mathbf{L}_\mathrm{H} - \mathbf{R}_\mathrm{H})] + \int \mathrm{d}\mathbf{S} \cdot \mathbf{D}^*(L_\mathrm{D} - R_\mathrm{D}) + \int \Phi^* \mathrm{d}\mathbf{S} \cdot \mathbf{L}_\Phi, \quad (11)$$

where $\mathrm{d}\mathbf{S}$ is the surface element of the surface surrounding the domain and directed outward. The volume integral part is:

$$Q_\mathrm{V} = \int \mathrm{d}V[\mathbf{A}^* \cdot \mathbf{L}'_\mathrm{A} + \mathbf{H}^* \cdot (\mathbf{L}'_\mathrm{H} - \mathbf{R}_\mathrm{H}) + \mathbf{D}^* \cdot (\mathbf{L}'_\mathrm{D} - \mathbf{R}'_\mathrm{D}) + \Phi^* L'_\Phi] \quad (12)$$

with

$$\mathbf{L}'_\mathrm{A} = \nabla \times \mathbf{L}_\mathrm{A} + ik_0\mathbf{L}_\Phi, \mathbf{L}'_\mathrm{H} = ik_0\mathbf{L}_\mathrm{A} + \nabla \times \mathbf{L}_\mathrm{H},$$
$$\mathbf{R}'_\mathrm{H} = \nabla \times \mathbf{R}_\mathrm{H}, \mathbf{L}'_\mathrm{D} = -ik_0\mathbf{L}_\mathrm{H} - \nabla L_\mathrm{D} - ik_0\hat{\boldsymbol{\zeta}}^{T*} \cdot \mathbf{L}_\Phi,$$
$$\mathbf{R}'_\mathrm{D} = -ik_0\mathbf{R}_\mathrm{H} - \nabla R_\mathrm{D}, L'_\Phi = -\nabla \cdot \mathbf{L}_\Phi$$

If **A, H, D** and Φ are the solutions of the system (5)–(8) Q_S is zero, while for arbitrary vectors **A, H, D** and Φ, Q_S could have any value. For further consideration we restrict the space of problems under consideration to those ones for which each integrand for each of four terms in (11) nullify (with $\mathbf{R}_\mathrm{H} = 0$ and $R_\mathrm{D} = 0$), i.e.:

$$\mathrm{d}\mathbf{S} \cdot (\mathbf{A}^* \times \mathbf{L}_\mathrm{A}) = 0,\ \mathrm{d}\mathbf{S} \cdot (\mathbf{H}^* \times \mathbf{L}_\mathrm{H}) = 0,\ \mathrm{d}\mathbf{S} \cdot \mathbf{D}^* L_\mathrm{D} = 0,\ \Phi^* \mathrm{d}\mathbf{S} \cdot \mathbf{L}_\Phi = 0, \quad (13)$$

and consider only problems for which at the domain surface:

$$R_D|_S = 0,\ \mathrm{d}\mathbf{S} \times \mathbf{R}_\mathrm{H}|_S = 0 \quad (14)$$

charge density and tangent current density nullify. However, the space of remaining problems remains rather wide and includes practically important tasks. In this way we achieve $Q_\mathrm{S} = 0$ for all arbitrary vectors from the restricted by (13) subspace including the solutions of the source system of equations (5)–(8).

We combine the quantities vectors **A, H, D** and Φ into one ten-component vector $\mathbf{X}$ and denote the corresponding ten-component operator by $\mathbf{L}$. With such a notation the volume integral is:

$$Q_\mathrm{V} = \int \mathrm{d}V \mathbf{X}^* \cdot \mathbf{L}(\mathbf{X}). \quad (15)$$

If the conditions (13), (14) are met for vectors $\mathbf{X}$, $Q_\mathrm{V} > 0$. This means, that operator $\mathbf{L}$ is positive.

The explicit form of the equations $\mathbf{L}(\mathbf{X}) = \mathbf{R}$ (where $\mathbf{R}$ is the combined right-hand side) is:

$$-\Delta\mathbf{A} + k_0^2\mathbf{A} - ik_0\nabla \times \mathbf{H} - k_0^2\hat{\boldsymbol{\zeta}} \cdot \mathbf{D} + ik_0\nabla\Phi = 0, \quad (16)$$

$$-\Delta\mathbf{H} + k_0^2\mathbf{H} + ik_0\nabla \times \mathbf{A} + ik_0\nabla \times \mathbf{D} = \frac{4\pi}{c}\nabla \times \boldsymbol{j}_\mathrm{ext}, \quad (17)$$

$$-\nabla\nabla \cdot \mathbf{D} + k_0^2(\mathbf{D} + \hat{\boldsymbol{\zeta}}^{*T} \cdot \hat{\boldsymbol{\zeta}} \cdot \mathbf{D}) - k_0^2\hat{\boldsymbol{\zeta}}^{*T} \cdot \mathbf{A} - ik_0\nabla \times \mathbf{H} - ik_0\hat{\boldsymbol{\zeta}}^{*T} \cdot \nabla\Phi = -ik_0\frac{4\pi}{c}\boldsymbol{j}_\mathrm{ext} - 4\pi\nabla\rho_\mathrm{ext}, \quad (18)$$

$$-\Delta\Phi + ik_0\nabla \cdot \mathbf{A} - ik_0\nabla \cdot \hat{\boldsymbol{\zeta}} \cdot \mathbf{D} = 0. \quad (19)$$

Here $(\hat{\boldsymbol{\zeta}}^{*T})_{ik} = (\hat{\boldsymbol{\zeta}})^*_{ki}$. In obtaining the above system, the formulas $\nabla \times \nabla \times \mathbf{A} = -\Delta\mathbf{A}$ and $\nabla \times \nabla \times \mathbf{H} = -\Delta\mathbf{H}$ have been used which follow from the Coulomb gauge applied on $\mathbf{A}$:

$$\nabla \cdot \mathbf{A} = 0 \quad (20)$$

and from the divergence-free property of $\mathbf{H}$:

$$\nabla \cdot \mathbf{H} = 0 \quad (21)$$

which is a consequence of (5). In this way the curl operator is deleted from the leading derivatives in the system (16)–(19). In addition, after such a transformation the dependency of equations which is inherited from the system (5)–(8) is now cancelled.

The system (16)–(19) supports the divergence-free property of $\mathbf{A}$ and $\mathbf{H}$ in the following way:

$$\Delta(\nabla \cdot \mathbf{A}) = 0, \quad (22)$$

$$\Delta(\nabla \cdot \mathbf{H}) - k_0^2(\nabla \cdot \mathbf{H}) = 0. \quad (23)$$

Each of these equations obtained from (16)–(19) is isolated and have no right-hand side. They have zero valued solutions when the appropriate boundary conditions are imposed to the system (16)–(19).

Some trouble comes from the leading order term $\nabla\nabla \cdot \mathbf{D}$ in equation (18). The gradient of divergence operator has a large zero-space consisting of curls of arbitrary vectors. So, after discretization, spurious modes may appear. This is maybe not possible to make an analytical analysis of the spurious modes for the general case which covers all geometries, discretization methods and mesh configurations. Anyway, such analysis

is made in the next section for the particular case considered there.

The requirement to the discretization applied to the system (16)–(19) is not only to reproduce the vector $\mathbf{X}$ by the vector of discrete values $\mathbf{x}$, the system of differential equations $\mathbf{L}(\mathbf{X}) = \mathbf{R}$ by the linear system $\mathrm{M}\mathbf{x} = \mathbf{b}$, but also to reproduce the integral $I = \int \mathrm{d}V \mathbf{X}^* \cdot \mathbf{Y}$ by the dot product $\tilde{I} = (\mathbf{x}, \mathbf{y}) = \sum_i x_i^* y_i$.

3. The numerical exercise

As a simple example, the problem of electromagnetic field distribution in the metallic rectangular cavity (parallelepiped) is analyzed. The boundaries of the cavity are: $x = 0$, $x = L_x$; $y = 0$, $y = L_y$; $z = 0$, $z = L_z$. The cavity is assumed to be empty with $\hat{\xi} = 1$. For the numerical solution we use the finite difference method. The coordinates are Cartesian, and the system (16)–(19) is projected to the coordinates. The mesh chosen is rectangular and equidistant. The mesh steps are $h_u = L_u/(N_u - 1)$, where u can be x, y, z; N_u are the numbers of the mesh nodes.

The differential operators are reproduced by the central differences.

3.1. Spurious modes

Spurious modes appear as perturbations over the regular solutions, and they are described by the discretized system (16)–(19) with zero right-hand side. The spurious modes are the result of discrepancy between differential and difference operators. This difference becomes visible for quickly oscillating solutions. The quickly oscillating solutions are described well within the WKB approximation. The WKB approach gives separate equations for the phase (eikonal) and amplitude of the solution. Since the analysis is for existence/non-existence of the spurious solutions, the treatment of the dispersion equation which is used to find the eikonal is sufficient. So, $f^{(i+1,j,k)} = f^{(i,j,k)} \exp(ik_x h_x)$, $f^{(i,j+1,k)} = f^{(i,j,k)} \exp(ik_y h_y)$ and $f^{(i,j,k+1)} = f^{(i,j,k)} \exp(ik_z h_z)$. Here f could be Φ and any component of **A, H** and **D**. The wavenumber then is $\mathbf{k} = (k_x, k_y, k_z)$. Since the wavelength is short ($k_u h_u \gg 1/(N_u - 1)$, $u = x, y, z$), the first terms in the discretized equations (16), (17) and (19), the terms with Laplasian operator, turn into dominant, and **A, H** and Φ become then negligibly small. The discretized equation (18) can be written as:

$$\boldsymbol{\kappa}\boldsymbol{\kappa} \cdot \mathbf{D} + 2k_0^2 \mathbf{D} + \hat{\mathbf{p}} \cdot \mathbf{D} = 0, \tag{24}$$

where $\kappa_u = \sin(k_u h_u)/h_u$ is the discrete representation of k_u, $\hat{\mathbf{p}}$ is the diagonal matrix with the following components: $p_{uu} = [1 - \cos(k_u h_u)]^2/h_u^2$. The 1st and 2nd terms in (24) represent the 1st and 2nd terms in (18). The last term of (24) is a creation of discretization. With $\mathbf{k} \to 0$, it goes to zero much faster then others, but for large wavenumbers it could be even dominant. The equation (24) prompts that the sum of the last two terms is collinear with vector $\boldsymbol{\kappa}$:

$$G\boldsymbol{\kappa} = 2k_0^2 \mathbf{D} + \hat{\mathbf{p}} \cdot \mathbf{D}, \tag{25}$$

where G is a constant. This formula is used to find **D**. Then **D** is substituted to (24) which results in the following dispersion equation:

$$\boldsymbol{\kappa} \cdot \hat{\mathbf{s}} \cdot \boldsymbol{\kappa} = -1, \tag{26}$$

where $\hat{\mathbf{s}}$ is a diagonal matrix in which $s_{uu} = 1/(2k_0^2 + p_{uu})$. Every component of the dot product in (26) is positive. This means that the dispersion equation has no real solutions and, the spurious modes do not exist.

3.2. Discretization procedure

In our numerical exercise the tangent current densities and the charge density, following to (14), nullifies at the boundary surface: $d\mathbf{S} \times \boldsymbol{j}_{\mathrm{ext}}|_S = 0$ and $\rho_{\mathrm{ext}}|_S = 0$.

The boundary conditions at the metallic surfaces are $d\mathbf{S} \times \mathbf{A}|_S = 0$, $d\mathbf{S} \times \mathbf{A}|_S = 0$, $d\mathbf{S} \cdot \mathbf{H}|_S = 0$, $\Phi|_S = 0$. How to handle with the vector components not covered by the above conditions is briefly explained in the appendix (available online at stacks.iop.org/PPCF/63/124007/mmedia).

3.3. Analytical solution

To analyze the numerical results it is good to have an analytical solution for further comparison.

The constructed analytical solution is the following.

The external current density is prescribed as:

$$\begin{aligned} \boldsymbol{j}_{\mathrm{ext}} = {} & \mathbf{e}_x j_{0x} \cos(k_x x) \sin(k_y y) \sin(k_z z) \\ & + \mathbf{e}_y j_{0y} \sin(k_x x) \cos(k_y y) \sin(k_z z) \\ & + \mathbf{e}_z j_{0z} \sin(k_x x) \sin(k_y y) \cos(k_z z) \end{aligned} \tag{27}$$

where $k_x = \pi/L_x$, $k_y = \pi/L_y$, $k_z = \pi/L_z$. j_{0x}, j_{0y} and j_{0z} are the constants. For such currents the analytical solutions are:

$$\begin{aligned} \mathbf{A} = {} & \mathbf{e}_x A_{0x} \cos(k_x x) \sin(k_y y) \sin(k_z z) \\ & + \mathbf{e}_y A_{0y} \sin(k_x x) \cos(k_y y) \sin(k_z z) \\ & + \mathbf{e}_z A_{0z} \sin(k_x x) \sin(k_y y) \cos(k_z z) \end{aligned} \tag{28}$$

with:

$$\mathbf{A}_0 = \frac{4\pi i k_0}{c(k^2 - k_0^2)} \left[\mathbf{j}_0 - \frac{\mathbf{k}(\mathbf{k} \cdot \mathbf{j}_0)}{k^2} \right]. \tag{29}$$

Magnetic field expression is:

$$\begin{aligned} \mathbf{H} = {} & \mathbf{e}_x H_{0x} \sin(k_x x) \cos(k_y y) \cos(k_z z) \\ & + \mathbf{e}_y H_{0y} \cos(k_x x) \sin(k_y y) \cos(k_z z) \\ & + \mathbf{e}_z H_{0z} \cos(k_x x) \cos(k_y y) \sin(k_z z) \end{aligned} \tag{30}$$

and

$$\mathbf{H}_0 = (\mathbf{k} \times \mathbf{A}_0)/(ik_0). \tag{31}$$

The potential is:

$$\Phi = \Phi_0 \sin(k_x x) \sin(k_y y) \sin(k_z z), \tag{32}$$

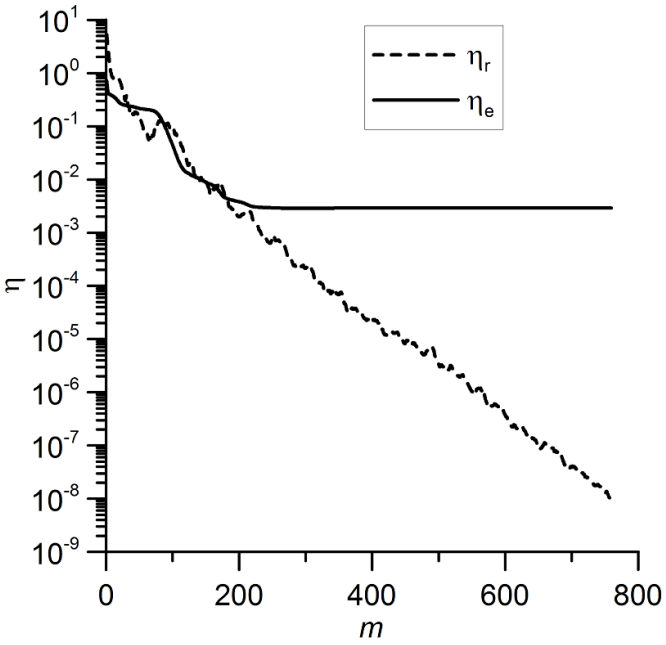

Figure 1. Convergence rate for mesh size $N = 41 \times 41 \times 41$ and calculation parameters $L_x = 1$ cm, $L_y = 1$ cm, $L_z = 2$ cm and $L_0 = 0.8$ cm ($k_0 = \pi/L_0$).

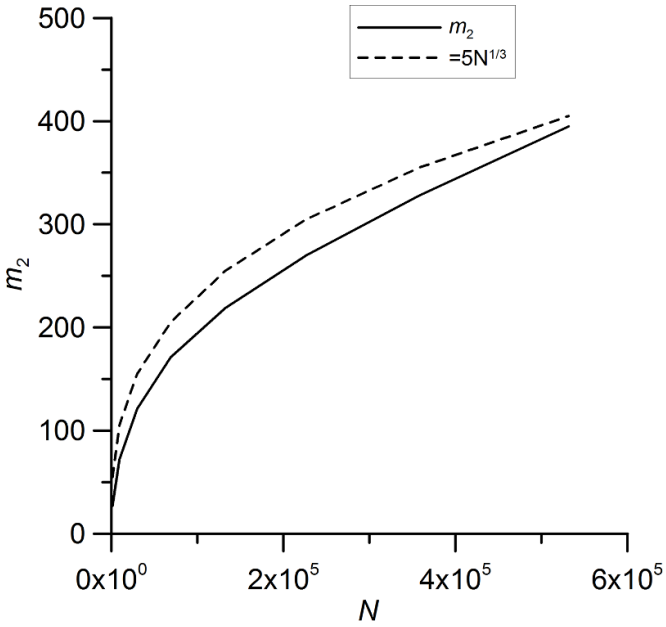

Figure 2. Optimum number of iterations m_2 as function of total number of mesh nodes N.

$$\Phi_0 = -\frac{4\pi}{ck_0^2}\mathbf{k}\cdot\mathbf{j}_0. \tag{33}$$

The electric displacement has a similar expression as (28) coefficients of which are calculated using the formula:

$$\mathbf{D}_0 = \mathbf{A}_0 + i\mathbf{k}\Phi_0/k_0. \tag{34}$$

3.4. Numerical results

After discretization, the resulting linear system $\mathbf{Mx} = \mathbf{b}$ is solved using the CGs method. No matrix preconditioning is employed. In the calculations, the normalized residual is computed:

$$\eta_r^{(m)} = \sqrt{\frac{(\mathbf{Mx}^{(m)} - \mathbf{b}, \mathbf{Mx}^{(m)} - \mathbf{b})}{(\mathbf{b}, \mathbf{b})}}. \tag{35}$$

Here m is enumerates iterations. The normalized error:

$$\eta_e^{(m)} = \sqrt{\frac{(\mathbf{x}^{(m)} - \mathbf{x}_a, \mathbf{x}^{(m)} - \mathbf{x}_a)}{(\mathbf{x}_a, \mathbf{x}_a)}} \tag{36}$$

is also calculated ($\mathbf{x}_a$ contains the analytical solution values in the mesh nodes). The test show rather quick and smooth convergence (see figure 1).

While the residual constantly (in average) decreases, the error saturates converging to the error value of the discretization scheme. It is expedient to stop iterations when the error is close to that value. Figure 2 shows the number of iterations m_2 needed to achieve twice less accuracy than the discretization offers as a function of total mesh node numbers N (in this numerical experiment mesh is scaled proportionally).

So, the optimum number of iterations scales close to $N^{1/3}$ which indicates a good performance of the iteration scheme.

In practice the analytical solution is not known. The optimum number of iterations could be determined either by detecting the saturation of iterations or using an estimate for the residual produced by the discretization template.

4. Conclusions

A new form of time-harmonic Maxwell's equations is developed and proposed for numerical modeling. It is written for the magnetic field strength **H**, electric displacement **D** and vector potential **A** and the scalar potential Φ. There are several attractive features of this form. The first is that the differential operator acting on these quantities is positive. This opens a door for usage, after discretization, of standard iterative procedure such as CGs. Second is absence of *curl* operators among leading order differential operators. The Laplacian stands for leading order operator in the equations for **H, A** and Φ and the gradient of divergence stands for **D**. This arrangement allows one to use the standard discretization procedure and use the same mesh for all quantities, and also facilitates the boundary condition applications. The 3rd feature is absence of space varied coefficients in the leading order differential operators that provides diagonal domination of the resulting matrix of the discretized equations.

The analysis of spurious modes showed their non-existence in case of regular mesh and finite differences usage.

A simple example is given to demonstrate the performance of time-harmonic Maxwell's equations; a 3D finite difference approach is used with the CGs method for iterations. Specifics of techniques of handling with boundaries are explained. In the example, quite good conversion of the iterations is achieved.

It is expected that this approach would have wide scope of usage. The only constraint is that equation (14) should be satisfied. This mean that problems with non-zero external charge density just at the boundary surface are not allowed. Also, the external currents at the surface directed along it are not allowed too. But the problems for which above requirements are not satisfied seem rather exceptional than practical. Within this approach, some complexity for imposing the boundary conditions exists, but is solvable. In this respect the finite element discretization procedure is expected to be much simpler.

Data availability statement

All data that support the findings of this study are included within the article (and any supplementary files).

Acknowledgments

This work has been carried out within the framework of the EUROfusion Consortium and has received funding from the Euratom research and training programme 2014–2018 and 2019–2020 under Grant Agreement No. 633053. The views and opinions expressed herein do not necessarily reflect those of the European Commission.

This work also received funding from National Academy of Sciences of Ukraine (Grants П-3-22, and Цв-5-20).

ORCID iDs

V E Moiseenko https://orcid.org/0000-0001-9431-5617
O Ågren https://orcid.org/0000-0001-5231-4392

References

[1] Yee K S 1966 *IEEE Trans. Antenna Propag.* **AP-14** 302–7
[2] Moiseenko V E and Ågren O 2006 *J. Plasma Phys.* **72** 1133–7
[3] Moiseenko V E and Ågren O 2005 *Phys. Plasmas* **12** 102504
[4] Moiseenko V E and Ågren O 2007 Second harmonic ion cyclotron heating of sloshing ions in a straight field line mirror *Phys. Plasmas* **14** 022503
[5] Appert K, Berger D, Gruber R and Rappaz J 1975 *J. Comput. Phys.* **18** 284–99
[6] Nédélec J C 1980 *Numer. Math.* **35** 315–41
[7] Saad Y 2003 *Iterative Methods for Sparse Linear Systems* (New York: PWS Publishing) (https://doi.org/10.1137/1.9780898718003)
[8] Moiseenko V E 2005 *Trans. Fusion Sci. Technol.* **47** 116–9
[9] Li D, Greif C and Schötzau D 2012 *Numer. Linear Algebra Appl.* **19** 525–39
[10] Aleynikov P and Marushchenko N B 2019 *Comput. Phys. Commun.* **241** 40–47